van der Waals model for the surface tension of liquid ^{4}He near the λ point

Paul Tavan* and B. Widom
Department of Chemistry, Cornell University, Ithaca, New York 14853
(Received 12 July 1982)

We develop a phenomenological model of the ^{4}He liquid-vapor interface. With it we calculate the surface tension of liquid helium near the λ point and compare with the experimental measurements by Magerlein and Sanders. The model is a form of the van der Waals surface-tension theory, extended to apply to a phase equilibrium in which the simultaneous variation of two order parameters—here the superfluid order parameter and the total density—is essential. The properties of the model are derived analytically above the λ point and numerically below it. Just below the λ point the superfluid order parameter is found to approach its bulk-superfluid-phase value very slowly with distance on the liquid side of the interface (the characteristic distance being the superfluid coherence length), and to vanish rapidly with distance on the vapor side, while the total density approaches its bulk-phase values rapidly and nearly symmetrically on the two sides. Below the λ point the surface tension has a $|\epsilon|^{3/2}$ singularity ($\epsilon \sim T - T_\lambda$) arising from the temperature dependence of the spatially varying superfluid order parameter. This is the mean-field form of the more general $|\epsilon|^\mu$ singularity predicted by Sobyanin and by Hohenberg, in which μ (which is in reality close to 1.35 at the λ point of helium) is the exponent with which the interfacial tension between two critical phases vanishes. Above the λ point the surface tension in this model is analytic in ϵ. A singular term $|\epsilon|^\mu$ may in reality be present in the surface tension above as well as below the λ point, although there should still be a pronounced asymmetry. The variation with temperature of the model surface tension is overall much like that in experiment.

I. INTRODUCTION

Liquid ^{4}He in equilibrium with its vapor undergoes its λ transition at $T_\lambda = 2.18$ K. Below the λ point it may be thought of as, and is thermodynamically equivalent to,[1] a three-phase system consisting of two "phases" β and γ making up the superfluid He II, and their common vapor α, as illustrated in Fig. 1(a). In contrast to other three-phase systems there is here only one interface separating both superfluid phases β and γ from the gas phase α and one corresponding surface tension σ:

$$\sigma = \sigma_{\alpha\beta} = \sigma_{\alpha\gamma} \ . \tag{1.1}$$

As shown in Fig. 1(b), the system above T_λ consists of only two phases, the vapor α and the He I liquid denoted by $\beta\gamma$. The λ point, therefore, is a critical endpoint of a three-phase equilibrium.

Magerlein and Sanders have measured[2,3] the liquid-vapor surface tension of ^{4}He as a function of temperature in the neighborhood of the λ point. The surface tension decreases with increasing temperature and shows a slight but distinct change of slope at T_λ (Fig. 2). Viewed on a coarse temperature scale this appears to be a discontinuity in slope, but on a finer scale the kink in σ vs T at T_λ is seen to be rounded. Magerlein and Sanders found that their data could be fitted reasonably well by

$$\sigma(\epsilon) = \sigma(0) - a\epsilon + b|\epsilon|^\mu \ , \tag{1.2}$$

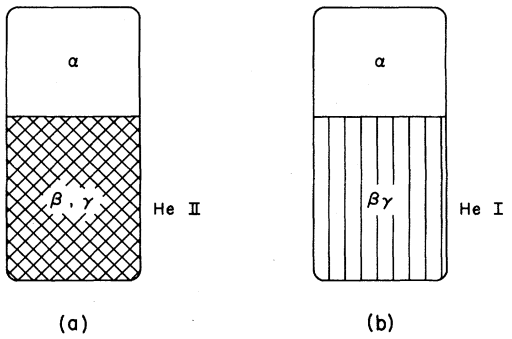

FIG. 1. Vapor (α) in equilibrium with (a) superfluid He II (phases β and γ) at $T < T_\lambda$, or (b) normal liquid He I (phase $\beta\gamma$) at $T > T_\lambda$.

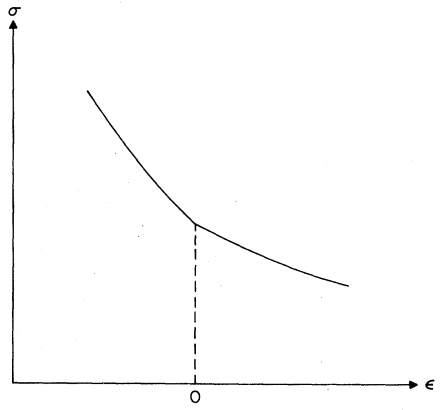

FIG. 2. Surface tension of liquid helium as a function of $\epsilon=(T-T_\lambda)/T_\lambda$; schematic.

where $\mu\approx 1.35$, a and b are positive parameters, and ϵ is the reduced temperature

$$\epsilon=\frac{T-T_\lambda}{T_\lambda}\ . \tag{1.3}$$

The form (1.2) of the temperature expansion of σ had been suggested by Sobyanin[4] on the basis of the Landau-Ginzburg-Pitaevskii theory and by Hohenberg[5] by scaling arguments. They agree that the singularity in the surface tension is of the form $|\epsilon|^\mu$, where $\mu=2-\nu-\alpha$. Here ν is the exponent that determines the rate of divergence of the coherence length of order-parameter fluctuations and α is the exponent of the specific-heat divergence. While Sobyanin predicted the singular term in (1.2) only for $T<T_\lambda$, Hohenberg argued that it should appear on both sides of the critical endpoint.

Here we take up the problem of the surface tension of liquid helium near its λ point and we also study the structure (density and order-parameter profile) of the liquid-vapor interface through the van der Waals,[6] Cahn-Hilliard theory[7] of fluid interfaces. In Sec. II we state the basic formulas of that theory and introduce the two order parameters x and y with which we characterize the phases. It was remarked earlier[8] that one must have at least two order parameters in the van der Waals theory since in a one-order-parameter theory phase α is always unsymmetrically related to β and γ, and (1.1) does not hold. The variable y will be related to the total density and x to the superfluid order parameter. We treat the latter as though it had only one component, and thus allow it only the two real values $\pm x_0$ in the bulk superfluid. In a more realistic model x would itself have two components, an amplitude, for example, and a phase angle, so that there would be a continuous infinity of superfluid phases, all with the same $|x|=x_0$, instead of only two.[1] That would present a more difficult problem, which we have not attempted to solve. It is an important open question how the present results would be altered if the superfluid order parameter were taken to have that more realistic symmetry. It is possible that the interfacial profiles would be significantly affected; but, since we know that many aspects of the thermodynamics and phase equilibria are realistically reproduced in the simpler model,[1] we are encouraged to believe that the surface tension may not be affected profoundly.

The description of our model is completed in Sec. III, where we specify the free-energy density as a function of x and y. In Sec. IV we present the analytical solution (within this van der Waals model) for the surface tension and the density profile at $T>T_\lambda$. Below the λ point such a solution is not possible. In Sec. V we analyze the asymptotic approach of the order-parameter profiles through the interface to their bulk superfluid values and determine the corresponding length scales. With these investigations as a basis, we construct in Sec. VI a numerical method suited to the calculation of the surface tension and of the density profiles in the critical region. In Sec. VII the numerical results are discussed, and an approximate expansion of the surface tension in powers of $|\epsilon|^{1/2}$ (characteristic of a mean-field theory) is derived and compared with the experimental findings. The concluding section, Sec. VIII, gives a brief summary and considers some possible implications of this work for the interpretation of the Magerlein-Sanders data.

II. OUTLINE OF THE THEORY

The state of liquid ^{4}He in equilibrium with its vapor is determined by only one thermodynamic field, which we may take to be the temperature, or the reduced temperature ϵ defined by (1.3). At given ϵ the various He phases are distinguished by the values of two order parameters x and y (Fig. 3). The super-

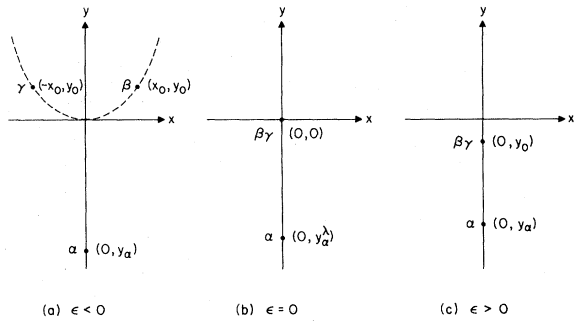

FIG. 3. Phases α, β, and γ, or α and $\beta\gamma$, in the plane of the order parameters x and y, for (a) $T<T_\lambda$ ($\epsilon<0$), (b) $T=T_\lambda$ ($\epsilon=0$), and (c) $T>T_\lambda$ ($\epsilon>0$).

fluid order parameter x is 0 in the bulk vapor, 0 in the bulk liquid when $\epsilon > 0$, and $\pm x_0$ ($x_0 > 0$) in the liquid phases when $\epsilon < 0$:

$$x_\beta = x_0, \quad x_\gamma = -x_0 \quad (x_0 > 0) . \tag{2.1}$$

The second order parameter y is, to within a positive, constant scaling factor c, the number density n relative to the density n_l^λ of the liquid at the λ point:

$$y = c(n - n_l^\lambda), \quad c > 0 . \tag{2.2}$$

The value of y in the bulk liquid phases is denoted by y_0; it is positive below the λ point ($y_\beta = y_\gamma = y_0 > 0$) and negative above ($y_{\beta\gamma} = y_0 < 0$). In the bulk gas phase y assumes a value $y_\alpha < 0$ which increases (becomes less negative) with increasing ϵ.

We extend the van der Waals, Cahn-Hilliard theory to this case of two order parameters. Let z be the distance in a direction perpendicular to the plane of the liquid-gas surface and taken to increase with increasing depth; i.e., to be the negative of the height. The order parameters x and y are assumed to vary smoothly with z through the interface from their values in the bulk gas ($z = -\infty$) to their values in the bulk liquid ($z = +\infty$). For the gas-superfluid α-β interface, therefore, when $\epsilon < 0$, the boundary conditions for the order-parameter profiles $x(z)$ and $y(z)$ are

$$(x,y) \rightarrow \begin{cases} (x_\beta, y_\beta) = (x_0, y_0), & z \rightarrow +\infty \\ (x_\alpha, y_\alpha) = (0, y_\alpha), & z \rightarrow -\infty \end{cases} \tag{2.3}$$

while for $\epsilon \geq 0$, i.e., for the α-$\beta\gamma$ interface,

$$(x,y) \rightarrow \begin{cases} (x_{\beta\gamma}, y_{\beta\gamma}) = (0, y_0), & z \rightarrow +\infty \\ (x_\alpha, y_\alpha) = (0, y_\alpha), & z \rightarrow -\infty . \end{cases} \tag{2.4}$$

The excess density $\omega(z)$ of grand-canonical free energy Ω (i.e., the excess over its value in a uniform fluid, where it is the negative of the pressure) is taken to be

$$\omega(z) = f[x(z), y(z)] + \tfrac{1}{2} m[\dot{x}(z)^2 + \dot{y}(z)^2] , \tag{2.5}$$

where dots denote differentiation with respect to z, where m, which we take to be a phenomenological parameter, is constant, and where $f(x,y)$ is the excess of the uniform pressure in the equilibrium bulk fluids over what would be the pressure if the fluid were constrained, hypothetically, to be uniform with values x and y of its order parameters, at given ϵ. This $f(x,y)$ is as given by a mean-field theory. It is 0 in the bulk phases,

$$f[x(\infty), y(\infty)] = f[x(-\infty), y(-\infty)] = 0 , \tag{2.6}$$

and positive everywhere else. In general, there would be a cross term $\dot{x}(z)\dot{y}(z)$ in (2.5), too, but for our present purpose, which is to outline the simplest phenomenological theory, that is an unnecessary refinement.

The equilibrium surface tension σ is the minimum over all possible profiles $x(z)$ and $y(z)$ of the integrated excess grand-canonical free energy per unit area:

$$\sigma = \min \int_{-\infty}^{+\infty} \omega(z) dz . \tag{2.7}$$

The equilibrium density profiles $x(z)$ and $y(z)$ through the interface are those that minimize the integral (2.7) and satisfy the boundary conditions (2.3) or (2.4). They may be obtained either from a numerical functional minimization of σ with respect to $x(z)$ and $y(z)$ or by integration of the corresponding Euler-Lagrange equations

$$m\ddot{x} = \frac{\partial f}{\partial x}, \quad m\ddot{y} = \frac{\partial f}{\partial y} . \tag{2.8}$$

With (2.6) these have as a first integral

$$\frac{m}{2}(\dot{x}^2 + \dot{y}^2) = f(x,y) \tag{2.9}$$

so with $x(z)$ and $y(z)$ the equilibrium profiles, the surface tension is also given by

$$\sigma = 2\int_{-\infty}^{+\infty} f[x(z), y(z)] dz \tag{2.10}$$

and by

$$\sigma = m \int_{-\infty}^{+\infty} (\dot{x}^2 + \dot{y}^2) dz . \tag{2.11}$$

Considering the equilibrium profiles $x(z)$ and $y(z)$ as a parametric representation of a trajectory $x(y)$ that links the respective bulk-phase points in the x-y plane, one may express (2.11) equivalently, using (2.9), as a path integral along the trajectory. Then the surface tension $\sigma_{\alpha\beta}$ of the gas-superfluid (α-β) interface, for example, is given by

$$\sigma_{\alpha\beta} = \sqrt{2m} \int_{y_\alpha}^{y_\beta} \sqrt{f[x(y), y]}\,[1 + x'(y)^2]^{1/2} dy , \tag{2.12}$$

where the prime means derivative with respect to y. The free-energy density $f(x,y) = f(x,y;\epsilon)$ and the profiles $x(z) = x(z;\epsilon)$ and $y(z) = y(z;\epsilon)$ depend parametrically on ϵ so the surface tension σ also depends on ϵ. Since the integral in (2.7) is stationary with respect to variations of the profiles about their equilibrium forms, we also have[9]

$$\frac{d\sigma}{d\epsilon} = \int_{-\infty}^{+\infty} \frac{\partial f}{\partial \epsilon} dz , \tag{2.13}$$

where the integral is to be evaluated with the equilibrium profiles $x(z)$ and $y(z)$ in $\partial f(x,y;\epsilon)/\partial\epsilon$.

III. MODEL FREE-ENERGY DENSITY

We take as a model free-energy density $f(x,y)$ a sixth-degree polynomial in x and y of the form

$$f(x,y)=f_0 f_1(x,y) f_2(x,y) , \tag{3.1}$$

with

$$f_1(x,y)=[x^2-y-(x_0^2-y_0)]^2+(y-y_0)^2 + 2(x-x_0)^2(x_0^2-y_0) , \tag{3.2}$$

$$f_2(x,y)=x^2+(y-y_\alpha)^2 , \tag{3.3}$$

and with f_0 some positive constant. For

$$x_0^2=y_0>0 \tag{3.4}$$

this $f(x,y)$ vanishes at three minima, one on the y axis at y_α and two located symmetrically with respect to the y axis on the parabola $x_0^2=y_0$ [cf. Fig. 3(a)]. The condition (3.4), therefore, defines the three-phase region; the minimum at $x=0$, $y=y_\alpha$ is associated with the α (vapor) phase and those at $x=\pm x_0$, $y=y_0$ are associated with the β and γ (superfluid) phases. When

$$x_0=0, \quad y_0\le 0 \tag{3.5}$$

the f of (3.1) has only two minima, both lying on the y axis, at y_0 and y_α, and corresponding to the liquid He I phase $\beta\gamma$ and the gas phase α [Figs. 3(b) and 3(c)]. In both the two- and three-phase regions f is an even function of x and therefore symmetric with respect to the y axis. In the three-phase region this symmetry [as we see, for example, from (2.12) and its analog for $\sigma_{\alpha\gamma}$] manifests itself in the required equality (1.1). It is sufficient in this region to calculate only the $\alpha\beta$ trajectory, the order-parameter profiles of the $\alpha\beta$ interface, and the surface tension $\sigma_{\alpha\beta}$, and then to identify these as the properties of the vapor-superfluid liquid interface.

The factor f_1 in (3.1) is given by (3.2) as a two-component (x and y) Landau expansion at a critical point. The coefficients of the terms linear in x and y, viz., $-4x_0(x_0^2-y_0)$ and $2(x_0^2-2y_0)$, are the respective thermodynamic fields conjugate to those densities. By symmetry, the former is 0 in any physically realizable state, so either $x_0=0$ ($\epsilon>0$) or $y_0=x_0^2$ ($\epsilon<0$), as in (3.4) and (3.5). The latter of the two fields, viz., the one conjugate to y, is the one physically variable field and, close to the λ point, may be identified with ϵ. Thus

$$x_0=0, \quad y_0=-\tfrac{1}{4}\epsilon \quad (\epsilon>0) \tag{3.6}$$

and

$$x_0=(-\tfrac{1}{2}\epsilon)^{1/2}, \quad y_0=-\tfrac{1}{2}\epsilon \quad (\epsilon<0) . \tag{3.7}$$

That the equilibrium bulk value x_0 of the superfluid order parameter vanishes proportionally to $(-\epsilon)^{1/2}$ as $\epsilon\to 0$ is a characteristic mean-field-theory result (critical-point exponent $\beta=\frac{1}{2}$, in conventional notation). The discontinuity in the derivative of y_0 with respect to ϵ at the critical point is analogous to the discontinuity in the constant-volume specific heat on the critical isochore that is characteristic of the mean-field theory of the critical point of liquid-vapor equilibrium; the density y here plays the role of the energy or entropy density at such a critical point. From (3.2), (3.6), and (3.7) the factor f_1 in f is

$$f_1(x,y;\epsilon)=x^4-2x^2y+2y^2+\epsilon y+\epsilon^2\gamma(\epsilon) , \tag{3.8}$$

where

$$\gamma(\epsilon)=\begin{cases}\frac{1}{4}, & \epsilon<0\\ \frac{1}{8}, & \epsilon>0 .\end{cases} \tag{3.9}$$

The vapor phase α is just a spectator to the $\beta\gamma$ critical point, so we take y_α to be simply linear in ϵ for small ϵ:

$$y_\alpha=y_\alpha^\lambda+q\epsilon , \tag{3.10}$$

where y_α^λ is the value of y_α at the λ point, and the constant q is imagined positive since the density of the vapor increases with increasing temperature. In all of our illustrations we shall take $q=-y_\alpha^\lambda=1$.

Figure 4 shows a contour plot of $f(x,y)/f_0$ at $\epsilon=-0.1$; i.e., far below the λ point. As ϵ increases towards the λ point the phase points β and γ move along the parabola $x^2=y$ towards the origin of the x,y plane, where they eventually merge into the single $\beta\gamma$ phase point. Above T_λ the $\beta\gamma$ phase point moves in the direction of more negative y as ϵ increases.

IV. SURFACE TENSION ABOVE THE λ POINT

Since f is symmetric with respect to the y axis, the first of the Euler-Lagrange equations (2.8) with the boundary conditions (2.4) has the trivial solution

$$x(z)\equiv 0 , \tag{4.1}$$

as expected. The interfacial free-energy density then depends only on the number-density profile $y(z)$; from (3.1)–(3.3) and (3.6)

$$f=2f_0(y-y_0)^2(y-y_\alpha)^2 . \tag{4.2}$$

With this f the second of Eqs. (2.8) may be solved analytically. With the boundary conditions (2.4) it yields the classical hyperbolic-tangent profile

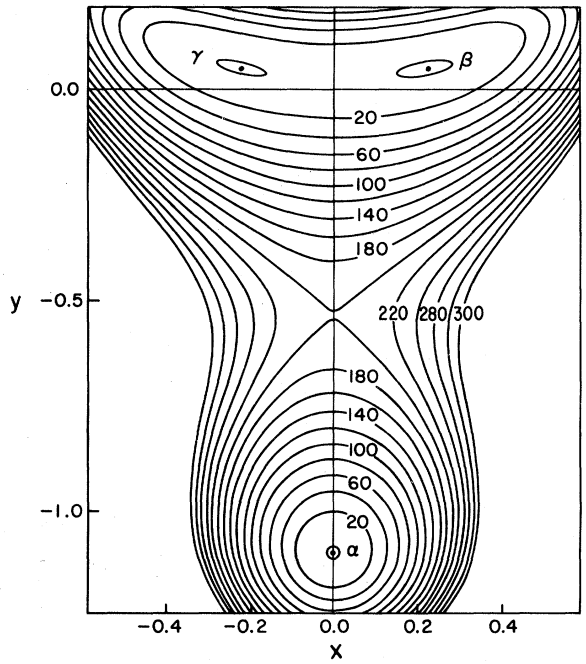

FIG. 4. Contours of constant $f(x,y)/f_0$ in the x,y plane for $q=-y_\alpha^\lambda=1$ and $\epsilon=-0.1$.

$$y(z)=\tfrac{1}{2}(y_0+y_\alpha)+\tfrac{1}{2}(y_0-y_\alpha)\tanh\frac{z}{2\xi}\ , \tag{4.3}$$

where ξ, the thickness of the interface, is given by

$$\xi^{-1}=2\left[\frac{f_0}{m}\right]^{1/2}(y_0-y_\alpha)\ . \tag{4.4}$$

We obtain the surface tension from (2.10), (2.11), or (2.12):

$$\sigma=\tfrac{1}{3}\sqrt{f_0 m}\,(y_0-y_\alpha)^3\ , \tag{4.5}$$

or, in terms of the temperature ϵ,

$$\sigma(\epsilon)=\sigma_0(1-d\epsilon)^3\ , \tag{4.6}$$

where σ_0 is the surface tension at the λ point

$$\sigma_0=\tfrac{1}{3}\sqrt{f_0 m}\,(-y_\alpha^\lambda)^3 \tag{4.7}$$

and where, from (3.6) and (3.10), the coefficient d is the positive constant

$$d=(q+\tfrac{1}{4})/(-y_\alpha^\lambda)\ . \tag{4.8}$$

For later comparison with the numerical results on the surface tension in the three-phase region it is useful to expand σ/σ_0 in powers of ϵ. Here we again take $q=-y_\alpha^\lambda=1$. Then from (4.6),

$$\sigma(\epsilon)/\sigma_0=1-3.75\epsilon+4.6875\epsilon^2-1.953\,125\epsilon^3\ . \tag{4.9}$$

V. LENGTH SCALES BELOW T_λ

The Euler-Lagrange equations (2.8) cannot be solved analytically with the free-energy density (3.1) in the three-phase region. We may gain some insight into the order-parameter profiles $x(z)$ and $y(z)$ by linearizing (2.8) in a small neighborhood of each of the bulk phases α and β. This will show us how the order parameters approach their bulk-phase values as $z\to\pm\infty$. Knowledge of this asymptotic behavior is prerequisite for the construction of a method of numerical solution. It will also allow us to determine analytically the shape and direction of the trajectory $x(y)$ close to its endpoints, as a test of the accuracy of the numerical results.

In the neighborhood $x_0+\xi$, $y_0+\eta$ of the β-phase point x_0, y_0, with the neglect of cubic and higher-order terms in ξ and η, the free-energy density (3.1) has elliptical contour lines (cf. Fig. 4) given by

$$2x_0^2\xi^2-2x_0\xi\eta+\eta^2=R^2 \tag{5.1}$$

and distinguished by the positive parameter R^2.

The principal axes of these ellipses define a coordinate system $\tilde\xi$, $\tilde\eta$ that is rotated by an angle K relative to the ξ,η coordinate system (cf. Fig. 5) with

$$\cot K=\frac{x_0}{x_0^2-\frac{1}{2}-\left[x_0^4+\frac{1}{4}\right]^{1/2}}\ . \tag{5.2}$$

Thus, as the λ point is approached from below, i.e., as $(x_0,y_0)\to(0,0)$, the short axis $\tilde\xi$ aligns itself more and more closely with the y axis of the x,y coordinate system. The ratio α of the lengths of the two principal axes,

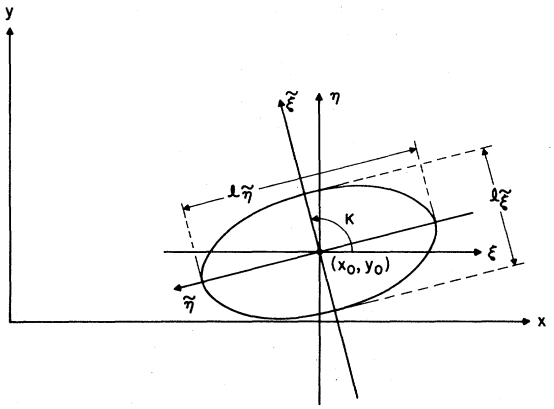

FIG. 5. Elliptical contour of constant $f(x,y)$ about the β-phase point x_0,y_0 in the order-parameter plane x,y. Coordinate systems ξ,η and $\tilde\xi,\tilde\eta$ have their origin at x_0,y_0 and are rotated from each other by the angle K. ξ and η axes are parallel to the x and y axes, respectively. $\tilde\xi$ and $\tilde\eta$ axes lie along the principal axes of the ellipse, which are of lengths $l_{\tilde\xi}$ and $l_{\tilde\eta}$, respectively.

$$\alpha=\frac{l_{\tilde{\eta}}}{l_{\tilde{\xi}}}=\left[\frac{x_0^2+\frac{1}{2}+(x_0^4+\frac{1}{4})^{1/2}}{x_0^2+\frac{1}{2}-(x_0^4+\frac{1}{4})^{1/2}}\right]^{1/2}, \tag{5.3}$$

then diverges due to a divergence of the length $l_{\tilde{\eta}}$ of the major axis. At the λ point the ellipse (5.1) degenerates into a pair of lines parallel to the x axis, indicating that the liquid-phase minimum of $f(x,y)$ has become quartic in the x direction while remaining quadratic in the y direction.

In the principal-axis coordinate system $\tilde{\xi},\tilde{\eta}$ the linearized Euler-Lagrange equations (2.8) are decoupled:

$$\ddot{\tilde{\xi}}=\xi_1^{-2}\tilde{\xi},\quad \ddot{\tilde{\eta}}=\xi_2^{-2}\tilde{\eta}\ , \tag{5.4}$$

where the constants ξ_1 and ξ_2 are

$$\xi_{1,2}^{-1}=2\{(f_0/m)[y_0+(y_0-y_\alpha)^2]\times[x_0^2+\tfrac{1}{2}\pm(x_0^4+\tfrac{1}{4})^{1/2}]\}^{1/2}\ . \tag{5.5}$$

We observe that the ratio ξ_2/ξ_1 is equal to the ratio α of the lengths of the principal axes of the ellipses (5.1). The constants ξ_1 and ξ_2 are, in fact, proportional to the lengths $l_{\tilde{\xi}}$ and $l_{\tilde{\eta}}$, respectively, and ξ_2 diverges as the λ point is approached from below. As will become apparent later, ξ_2 is the distance over which x decays through the surface from its bulk-phase value x_0 in the superfluid to 0 in the gas phase; i.e, it is the coherence length of the superfluid order parameter. The length ξ_1 remains finite and at T_λ becomes equal to ξ of Eq. (4.4), which is the distance over which the density varies between its two bulk-phase values. From (3.6) and (3.10), we may express ξ_2 as a function of the reduced temperature ϵ. For $|\epsilon|$ small

$$\xi_2^{-1}=\sqrt{-\epsilon}\,\sqrt{2f_0/m}\left[-y_\alpha^\lambda-\epsilon\left[q+\tfrac{3}{4}-\frac{1}{4y_\alpha^\lambda}\right]+O(\epsilon^2)\right]. \tag{5.6}$$

From (5.6) we see that ξ_2 diverges with the classical critical-point exponent $\nu=\frac{1}{2}$.

Imposing the boundary conditions (2.3), which imply that $\tilde{\xi}$ and $\tilde{\eta}$ vanish as $z\to\infty$, we find for the linearized differential equations (5.4), in the $(-,+)$ quadrant of the $\tilde{\xi},\tilde{\eta}$ coordinate system, the solutions

$$\tilde{\xi}(z)=-a\exp(-z/\xi_1)\ ,\qquad \tilde{\eta}(z)=b\exp(-z/\xi_2)\ , \tag{5.7}$$

where a and b are positive constants. According to (5.2) and (3.7), near criticality $\cot K\approx -x_0$. Transformation of the solutions (5.7) to the x,y coordinate system then yields for the profiles in the limit of large z,

$$x(z)\approx x_0[1+a\exp(-z/\xi_1)-(b/x_0)\exp(-z/\xi_2)]\ , \tag{5.8}$$

$$y(z)\approx y_0-a\exp(-z/\xi_1)-x_0 b\exp(-z/\xi_2)\ . \tag{5.9}$$

Since $\xi_2\gg\xi_1$ close to T_λ, the approach of either order parameter x or y towards its bulk-superfluid value will eventually be dominated by the slowly decaying exponential.

There is, however, an important difference between the two profiles, which is due to the different temperature dependence of the amplitudes of the exponentials. The solutions (5.8) and (5.9) have to hold in the limit $\epsilon=0$, where the superfluid order parameter $x(z)$ vanishes identically. Thus the integration constant b must also vanish in this limit, and we may anticipate that it does so proportionally to x_0. The integration constant a, on the other hand, must approach the value $-\frac{1}{2}y_\alpha^\lambda>0$ for $y(z)$ to approach the limiting profile (4.3). Therefore, the coefficients of the two exponentials in (5.8) are comparable, and, because the sign of the first is positive, most of the increase of $x(z)$ towards its bulk superfluid value x_0 occurs over the distance ξ_2. Meanwhile, close to the λ point the amplitude of the slowly decaying exponential in (5.9) is very small, so most of the increase of the particle density $y(z)$ towards its liquid-phase value occurs over the small distance ξ_1 while the additional increase of $y(z)$, which occurs over the longer distance ξ_2, becomes negligible as $\epsilon\to 0$. Therefore, two vastly different length scales are necessary for the description of the density profiles $x(z)$ and $y(z)$. This is the main difficulty in any attempt to calculate the surface tension numerically with sufficient accuracy in the three-phase region at temperatures close to T_λ. In Sec. VI we give a method that incorporates the length scales ξ_1 and ξ_2 from the outset and yields an accurate numerical solution.

The qualitative correctness of the numerical solutions can be judged by comparing the shape and direction of the trajectory $y(x)$ in the neighborhood of the bulk-phase points with the results of the asymptotic analysis. From (5.7) we obtain for the trajectory in the vicinity of the β-phase point in the principal-axis coordinate system $\tilde{\xi},\tilde{\eta}$

$$\tilde{\eta}=0\quad (b=0) \tag{5.10}$$

and

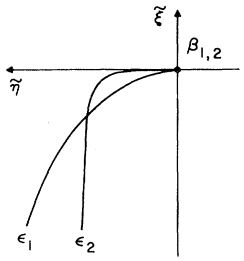

FIG. 6. Trajectory $\tilde{\xi}=-a(\tilde{\eta}/b)^{\alpha}$ for $\epsilon=\epsilon_1$ or $\epsilon=\epsilon_2$, with $-\epsilon_1>-\epsilon_2>0$, in the neighborhood of the β-phase point β_1 or β_2; schematic.

$$\tilde{\xi}(\tilde{\eta})=-\frac{a}{b^{\alpha}}\tilde{\eta}^{\alpha} \quad (b>0) \tag{5.11}$$

where α, given by (5.3), is the ratio ξ_2/ξ_1 of the two characteristic lengths. Below the λ point, where $b>0$, the trajectory approaches the β-phase point tangentially to the long axis of the elliptical contour because $\alpha>1$. As the critical endpoint is approached the exponent α and the factor a/b^{α} both diverge, so the trajectory clings more and more closely to the long axis, curving off from it more and more sharply towards the short axis (Fig. 6).

A similar analysis may be made of the approach of the profiles $x(z)$ and $y(z)$ to their respective gas-phase values 0 and y_{α} as $z\to-\infty$. It proves to be much simpler since the contour lines of the free-energy density $f(x,y)$ are circular in the vicinity of the α-phase point, thus yielding only one characteristic length ξ_{α}, of short range, $\xi_{\alpha}\approx\xi_1$: Both order parameters approach their bulk-gas-phase values on the same length scale ξ_1.

VI. NUMERICAL METHOD (REF. 10)

We calculate the surface tension in the three-phase region in the temperature range $0.0001\le-\epsilon\le0.1$ by a direct numerical functional minimization of the surface-tension integral (2.7) with respect to the profiles $x(z)$ and $y(z)$. This temperature range corresponds to the range $3.7\le\alpha\le115.4$ of the ratio of coherence lengths, $\alpha=\xi_2/\xi_1$ [see (5.3)], indicating that our calculations go deep into the critical region. To enable us to impose the boundary conditions (2.3) on the profiles and incorporate the vastly different length scales ξ_1 and ξ_2 into the theory we map the z axis onto a finite interval $I=[-1,\ b>1]$ by the following construction.

First we compress the z axis to the interval $I^A=[-1,1]$ by a change of integration variable from z to a variable s^A defined by

$$s^A=\tanh\frac{\tau z}{2\xi_1}\ , \tag{6.1}$$

where τ is some positive constant close to 1. Then we divide I^A into n^A+1 equal intervals, thus defining a grid A of points s_i^A, $i=0,1,\ldots,n^A+1$, where s_0^A and $s_{n^A+1}^A$ correspond to $z=-\infty$ and $z=+\infty$, respectively. The point $s_{n^A}^A$ corresponds to a value of z given by

$$z_{n^A}=(\xi_1/\tau)\ln n^A\ . \tag{6.2}$$

Thus any function of z that essentially varies between its two asymptotic values in an interval of order ξ_1 about $z=0$ varies smoothly and moderately on the grid A, which is then well suited to a numerical representation of the function.

To describe functions whose essential variations are over a greater range, ξ_2, occurring mostly at $z>z_{n^A}$, we replace the integration variable z in the interval $[z_{n^A},+\infty]$ by

$$s^B=b\tanh\frac{z}{2\bar{\xi}_2}\ , \tag{6.3}$$

where $\bar{\xi}_2\approx\xi_2$, and we choose a number n^X of grid points on which we are going to describe the profiles for $z\ge z_{n^A}$. Equation (6.3) compresses the z axis into an interval $I^B=[-b,b]$, which we then divide into n^B+1 equal intervals (grid B), in such a way that the next-to-last point $s_{n^A}^A$ of the grid A coincides with the point $s_{n^B-n^X}^B$ of the grid B (so that their respective transforms z_{n^A} and $z_{n^B-n^X}$ are therefore also equal). Fixing $\bar{\xi}_2(\approx\xi_2)$ determines the total number n^B of points on the grid B since

$$z_{n^B-n^X}=\bar{\xi}_2\ln\frac{n^B-n^X}{n^X+1}\ . \tag{6.4}$$

The condition $z_{n^A}=z_{n^B-n^X}$ then sets the size of the interval I^B,

$$b=\frac{(n^B+1)(n^A-1)}{[2(n^B-n^X)-(n^B+1)](n^A+1)}\ . \tag{6.5}$$

Thus we describe a function $g(z)$ for $z\le z_{n^A}$ as a function $g(s^A)$ on the points s_i, $i=0,\ldots,n_A$ of the A grid and for $z>z_{n^A}$ as a function $g(s^B)$ on the points s_i, $i=n^A+1,\ldots,n^A+n^X+1$ of the B grid. The boundary conditions are imposed at $s_0=-1$ and $s_{n+1}=b$, where $n=n^A+n^X$ is the total number of interior points.

With these definitions the surface-tension integral (2.7) can be represented as a sum of integrals over the compressed space:

$$\sigma=\int_{-1}^{s_{nA}}\frac{f(s^A)2\xi_1}{\tau[(1-(s^A)^2]}ds^A+\int_{-1}^{s_{nA}}\frac{k(s^A)[1-(s^A)^2]\tau}{2\xi_1}ds^A+\int_{s_{nA}}^{b}\frac{f(s^B)2b\bar{\xi}_2}{[b^2-(s^B)^2]}ds^B+\int_{s_{nA}}^{b}\frac{k(s^B)[b^2-(s^B)^2]}{2b\bar{\xi}_2}ds^B\,, \tag{6.6}$$

where $k(s)$ is the square-gradient term in (2.5) with the derivatives taken with respect to s. Each of these integrals is now replaced by a sum of integrals over intervals I_i of length h that bracket the points s_i and cover the whole compressed space I. Neglecting the two end intervals, where $\omega(s)$ is small, and assuming that the profiles and their derivatives vary slowly in each interval, we transform (6.6) into a functional of the profiles $x_i=x(s_i)$ and $y_i=y(s_i)$:

$$\sigma(\epsilon;n)=\sum_{i=1}^{n}(f_iv_i+k_iw_i)\,, \tag{6.7}$$

where

$$f_i=f(x_i,y_i)\,, \tag{6.8}$$

$$k_i=[\Delta^5(x_i)]^2+[\Delta^5(y_i)]^2\,, \tag{6.9}$$

with Δ^5 indicating a five-point difference, and where the weights v_i and w_i for the A grid, for instance, are the constants ($i=1,\ldots,n_A-1$),

$$v_i=\frac{2\xi_1}{\tau}\int_{I_i}\frac{ds}{1-s^2}\,, \tag{6.10}$$

$$w_i=\frac{m\tau}{4\xi_1(12h^A)^2}\int_{I_i}(1-s^2)ds\,. \tag{6.11}$$

Special precautions have to be taken at the point s_{nA}, where the two grids are linked. The boundary conditions enter at the two ends, through the differences (6.9). Given trial profiles x_i^0 and y_i^0, the functional (6.7) may now be minimized with respect to the $2n$ points x_i,y_i by standard procedures.

The resulting profiles were insensitive to the initial guesses x_i^0,y_i^0. They were also insensitive to the number n of points chosen, but for the surface tensions to be accurate, n had to be large: 500–1200, say, with $n^A\simeq 2n^X$. Computing times were only of the order of minutes even for very large n and poor initial guesses. To judge the accuracy of the minimized $\sigma(\epsilon;n)$ we also calculated σ by (2.10) and (2.11), thereby obtaining values $\sigma_f(\epsilon;n)$ and $\sigma_k(\epsilon;n)$ of which $\sigma(\epsilon;n)$ is the arithmetic mean. For our algorithm, with $\tau\leq 0.7$ [see (6.1)], we always had $\sigma_f(\epsilon;n)<\sigma_k(\epsilon;n)$.[11] We also found $\sigma_k(\epsilon;n)$ to be a monotonically decreasing and $\sigma_f(\epsilon;n)$ a monotonically increasing function of n, thus yielding monotonic upper and lower bounds for $\sigma(\epsilon;\infty)$, the asymptotic numerical result. The difference of the bounds, which we denote $\Delta\sigma(\epsilon;n)$, is an error bound.

For our two temperatures $\epsilon=-10^{-4}$ and $\epsilon=-5\times10^{-4}$ closest to the λ point, where the highest accuracy was required, and for $\epsilon=0$, where the analytical solution is known, we carried out an asymptotic analysis ($n\to\infty$) for our algorithm. For large n the surface tension $\sigma(\epsilon;n)$ proved to converge to the limiting (extrapolated) value $\sigma(\epsilon;\infty)$ as n^{-2}. From an analysis of the extrapolation procedure we determined an absolute error bound $\Delta\sigma(\epsilon;\infty)$ for the extrapolated $\sigma(\epsilon;\infty)$. Using up to $n=500$ grid points we obtained at $\epsilon=0$ the values

$$\sigma(0;\infty)/\sigma_0=1.0+1.5\times10^{-10}$$

and

$$\Delta\sigma(0;\infty)/\sigma_0=1.2\times10^{-9}\,,$$

TABLE I. Surface tension σ and its temperature derivative $d\sigma/d\epsilon$, from numerical minimization of the surface-tension integral, as functions of the reduced temperature $\epsilon<0$.

ϵ	n	$\sigma(\epsilon;n)/\sigma_0$	$\Delta\sigma(\epsilon;n)/\sigma_0$	$\frac{1}{\sigma_0}d\sigma(\epsilon;n)/d\epsilon$
0.0	∞	1.000 000 000	0.000 000 001	−3.750 000
−0.0001	∞	1.000 375 758	0.000 000 004	−3.761 557[a]
−0.0005	∞	1.001 884 086	0.000 000 118	−3.778 442[a]
−0.0010	900	1.003 777 639	0.000 002 196	−3.792 999
−0.0050	900	1.019 119 553	0.000 001 990	−3.872 847
−0.0100	600	1.038 688 158	0.000 004 382	−3.952 772
−0.0200	600	1.078 944 372	0.000 004 858	−4.096 543
−0.0400	600	1.163 585 438	0.000 014 680	−4.365 670
−0.0600	500	1.253 533 342	0.000 029 000	−4.629 078
−0.0800	500	1.348 750 580	0.000 045 940	−4.893 090
−0.1000	500	1.449 274 639	0.000 069 490	−5.160 015

[a]Calculated at $n=1200$.

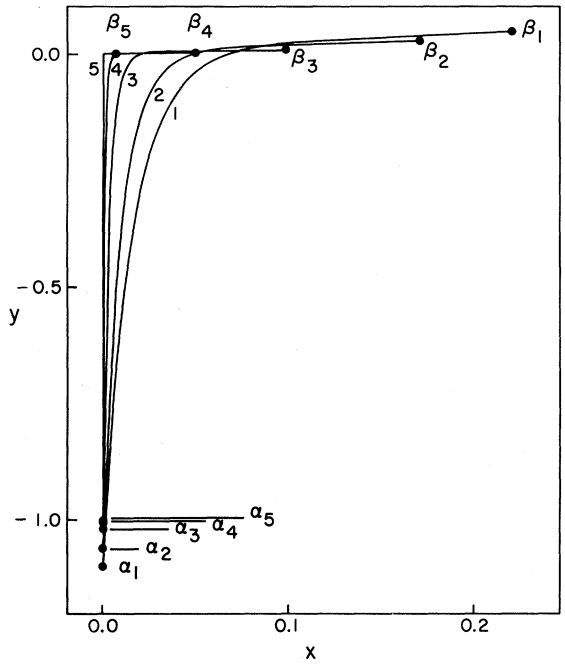

FIG. 7. Trajectories giving the variations of the order parameters x and y through the interface between the vapor α and the superfluid phase β, for (1) $\epsilon=-0.1$, (2) $\epsilon=-0.06$, (3) $\epsilon=-0.04$, (4) $\epsilon=-0.005$, and (5) $\epsilon=-0.0001$. Respective bulk-phase points are α_i and β_i.

demonstrating the accuracy of the numerical method.

VII. SURFACE TENSION BELOW THE λ POINT

The results of our numerical calculations are summarized in Table I, which gives the surface tensions $\sigma(\epsilon;n)$, the error bounds $\Delta\sigma(\epsilon;n)$, and the temperature derivatives $d\sigma(\epsilon;n)/d\epsilon$, the latter calculated from (2.13) with the profiles $x(z)$ and $y(z)$. Figure 7 shows a selection of trajectories $x(y)$. Starting at the gas-phase point α these follow the y axis more and more closely, and to smaller and smaller values of $|y|$, as $|\epsilon|$ decreases. The suddenness with which they ultimately veer away from the y axis towards $x>0$ also increases with decreasing $|\epsilon|$. On the scale of the figure, trajectory 5, corresponding to $|\epsilon|=10^{-4}$, seems to coincide with the y axis all the way to $y=0$, where it suddenly turns 90° and then follows the x axis to β_5. The actual deviations of that trajectory from the axes and the rounding of the turn are detectable only on a greatly expanded scale. We have taken $q=-y_\alpha^\lambda=1$ in all calculations.

The form of the trajectories in the neighborhood of the bulk-superfluid-phase points β is seen to agree well with the predictions of the asymptotic analysis

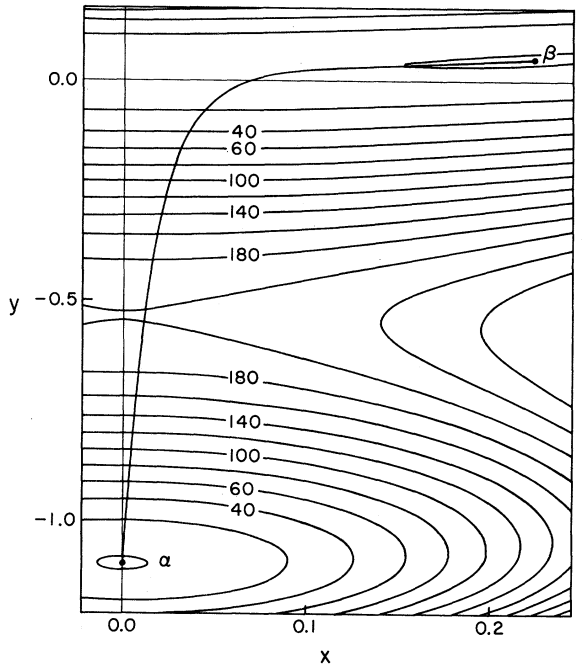

(a)

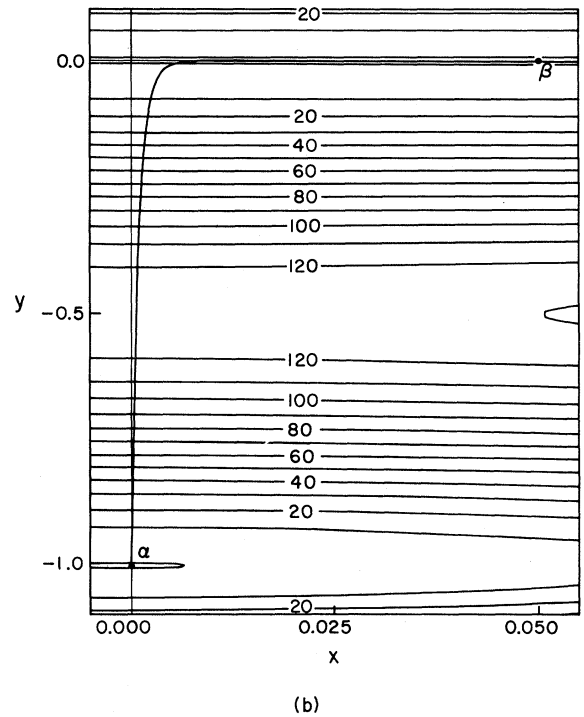

(b)

FIG. 8. x,y trajectory on a background of contour lines of constant $f(x,y)/f_0$, for (a) $\epsilon=-0.1$ and (b) $\epsilon=-0.005$. (Elliptical contour about the α-phase point would have been circular had the x and y scales been the same.)

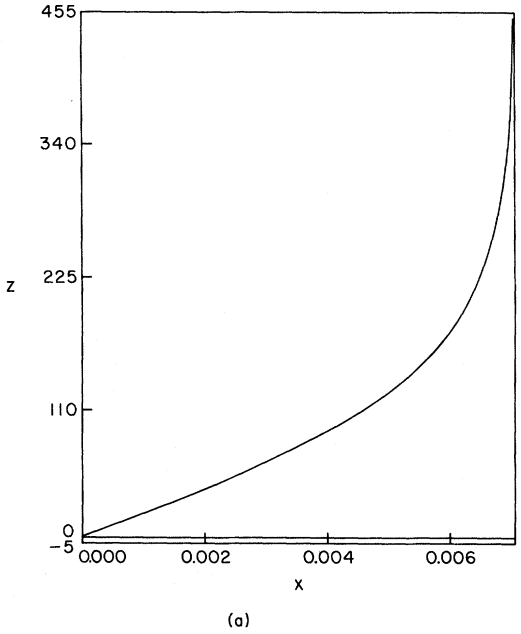

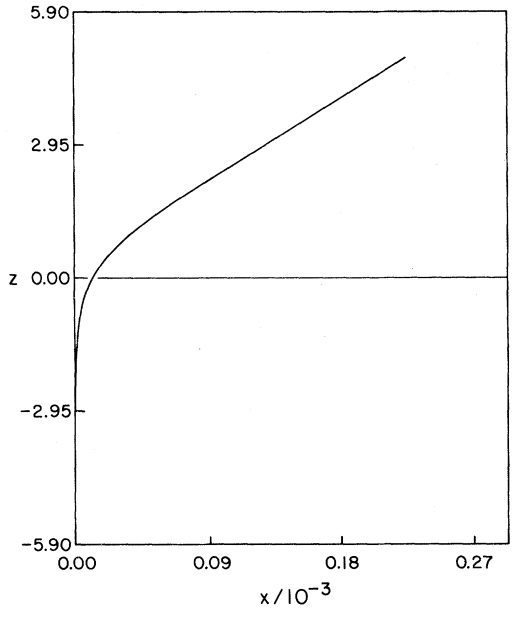

FIG. 9. Order parameter x as a function of distance z through the liquid-vapor interface near the λ point ($\epsilon = -10^{-4}$). Distance z is in units of $\sqrt{m/f_0}$. Scales are chosen to show (a) the slow decay of x to x_0 in the superfluid and (b) the rapid decay of x to 0 in the vapor.

summarized in Fig. 6. To examine this further, in Figs. 8(a) and 8(b) we display trajectories 1 and 4 on contour maps of the free-energy density $f(x,y;\epsilon)$. Both figures show that the trajectories do approach the β point tangentially to the long axes of the elliptical contours about this point. In Fig. 8(b) those ellipses seem already to have degenerated to pairs of straight lines. The direction of the tangent of $x(y)$ at β that we find numerically agrees closely with (5.2).

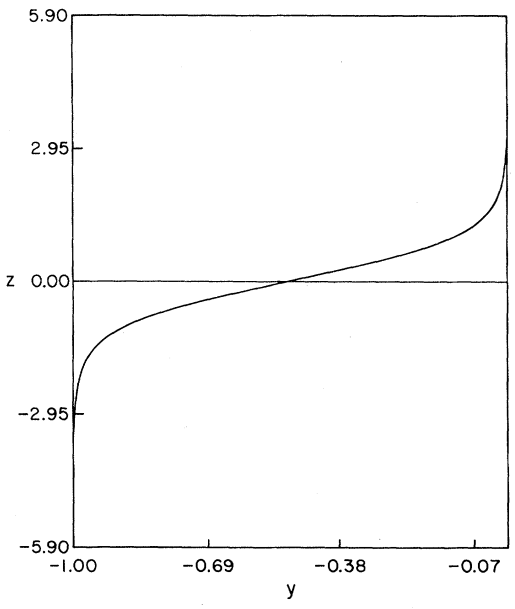

FIG. 10. Density y as a function of distance z (in units of $\sqrt{m/f_0}$) near the λ point ($\epsilon = -10^{-4}$).

Figures 9 and 10 give some insight into the structure of the surface of He II near the λ point. The figures show the profiles of the order parameters x and y as functions of the distance z through the interface for $\epsilon = -10^{-4}$. The profile of the superfluid order parameter x (Fig. 9) is highly asymmetric; x approaches its bulk-superfluid value x_0 at $z = +\infty$ very slowly, over several hundred units of z, while it decays to zero rapidly in the gas phase α as $z \to -\infty$ [Fig. 9(b)]. Numerically, for small $|\epsilon|$ the x profile is to a good approximation

$$x(z) \approx \tilde{x}(z) = \begin{cases} 0, & z \leq 0 \\ x_0 \tanh(z/2\xi_2), & z \geq 0 \end{cases} . \tag{7.1}$$

This confirms the conclusion in Sec. V that the ξ_2 of (5.5) may be identified with the coherence length of the superfluid order parameter.

As is apparent in Fig. 10, the density changes on a much smaller length scale. Although for the density, too, there is a slow, decay on the scale ξ_2, into the superfluid phase, this is not visible in the figure, since this slowly decaying part is only a fraction of order $|\epsilon| = 10^{-4}$ of the total change in density. Thus the y profile is nearly symmetric; it yields a sharp interface of thickness ξ given by (4.4), and it is well approximated by the hyperbolic-tangent profile (4.3), which we shall call $\tilde{y}(z)$.

TABLE II. Surface tension σ, the approximation $\tilde{\sigma}$, the contributions $\tilde{\sigma}_x$ and $\tilde{\sigma}_y$ to $\tilde{\sigma}$ made by the x and y profiles, the numerical error $\Delta\sigma$ in σ, and the difference $\sigma-\tilde{\sigma}$ between the exact and approximate surface tensions.

ϵ	$\tilde{\sigma}_y/\sigma_0$	$\tilde{\sigma}_x/\sigma_0$	$\tilde{\sigma}/\sigma_0$	σ/σ_0	$\Delta\sigma/\sigma_0$	$(\sigma-\tilde{\sigma})/\sigma_0$
0.0	1.000 000 000	0.0	1.000 000 000	1.000 000 000	0.000 000 001	0.0
−0.0001	1.000 375 047	0.000 000 707	1.000 375 754	1.000 375 758	0.000 000 004	0.000 000 004
−0.0005	1.001 876 172	0.000 007 914	1.001 884 086	1.001 884 086	0.000 000 118	0.000 000 000
−0.0010	1.003 754 687	0.000 022 405	1.003 777 093	1.003 777 639	0.000 002 196	0.000 000 546
−0.0050	1.018 867 184	0.000 252 500	1.019 119 683	1.019 119 553	0.000 001 990	−0.000 000 130
−0.0100	1.037 968 756	0.000 721 249	1.038 690 005	1.038 688 158	0.000 004 382	−0.000 001 847
−0.0200	1.076 874 998	0.002 080 000	1.078 954 998	1.078 944 372	0.000 004 858	−0.000 010 626
−0.0400	1.157 499 996	0.006 109 402	1.163 609 399	1.163 585 438	0.000 014 680	−0.000 023 961
−0.0600	1.241 874 994	0.011 639 381	1.253 514 375	1.253 533 342	0.000 029 000	0.000 018 967
−0.0800	1.329 999 925	0.018 559 994	1.348 559 919	1.348 750 580	0.000 045 940	0.000 190 661
−0.1000	1.421 875 112	0.026 832 826	1.448 707 938	1.449 274 639	0.000 069 490	0.000 566 700

Through (2.11) these two approximations $\tilde{x}(z)$ and $\tilde{y}(z)$ to the profiles allow us to write a corresponding approximation formula for the surface tension,

$$\sigma\sim\tilde{\sigma}=\tilde{\sigma}_x+\tilde{\sigma}_y\ , \tag{7.2}$$

which is expected to be asymptotically exact in the limit $|\epsilon|\to 0$. Here $\tilde{\sigma}_y$ is given by what was the analytical solution (4.5) above the λ point, while $\tilde{\sigma}_x$ is found to be

$$\tilde{\sigma}_x=\tfrac{1}{3}mx_0^2/\xi_2\ . \tag{7.3}$$

Expanding $\tilde{\sigma}$ in powers of ϵ and neglecting higher-order terms, we get from (4.9), (3.7), and (5.6)

$$\tilde{\sigma}(\epsilon)/\sigma_0=1.0-3.75\epsilon+\frac{1}{\sqrt{2}}|\epsilon|^{3/2}$$
$$+4.6875\epsilon^2+\sqrt{2}\,|\epsilon|^{5/2}\ . \tag{7.4}$$

The terms with fractional powers of $|\epsilon|$ are contributed by $\tilde{\sigma}_x$. They are not present above the λ point. The terms with integer exponents derive from the density profile $y(z)$ and are identical on both sides of the λ point. We shall call $\tilde{\sigma}_y$ the regular and $\tilde{\sigma}_x$ the singular part of the surface tension.

In Table II the numerical results for σ are compared with the approximation in (7.2) and (7.4). For $|\epsilon|\leq 10^{-2}$ they agree within the uncertainty $\Delta\sigma(\epsilon;n)$ in the numerical results. For larger values of $|\epsilon|$ deviations are unambiguous and increasing, indicating that (7.4) is correct only asymptotically for small $|\epsilon|$.

Having displayed the singular and regular contributions to σ separately in Table II, we can now also see why it was necessary to calculate σ for $|\epsilon|$ at least as small as 10^{-4} if we were to prove the correctness of the first singular term in the expansion (7.4). The reason is that successive contributions to σ differ by a factor of $|\epsilon|^{1/2}$, so it is only for such small $|\epsilon|$ that they differ in at least two decimal places and can be sorted out. The correctness of the first two (regular) terms follows from the continuity of σ and of its temperature derivative at $\epsilon=0$, which are expected on theoretical grounds[12] and which are clearly reflected in our numerical data. It is the unambiguous existence of a contribution of the order 0.7×10^{-6} to σ at $|\epsilon|=10^{-4}$, which cannot be attributed to a higher-order term, that proves the correctness of the $|\epsilon|^{3/2}$ term in the expansion (7.4). This justifies *a posteriori* the considerable effort that had to be made to obtain such accurate results near T_λ.

Figure 11 shows the approximation (7.4) to the

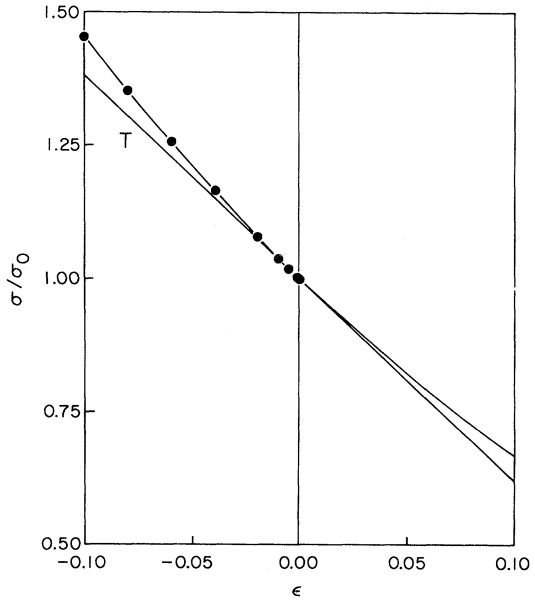

FIG. 11. σ/σ_0 as a function of ϵ. Line marked T is the tangent to the curve at the λ point. Circles are the numerical data, the branch of the curve at $\epsilon<0$ is the approximation $\tilde{\sigma}/\sigma_0$, and the branch of the curve at $\epsilon>0$ is the analytical solution for σ/σ_0.

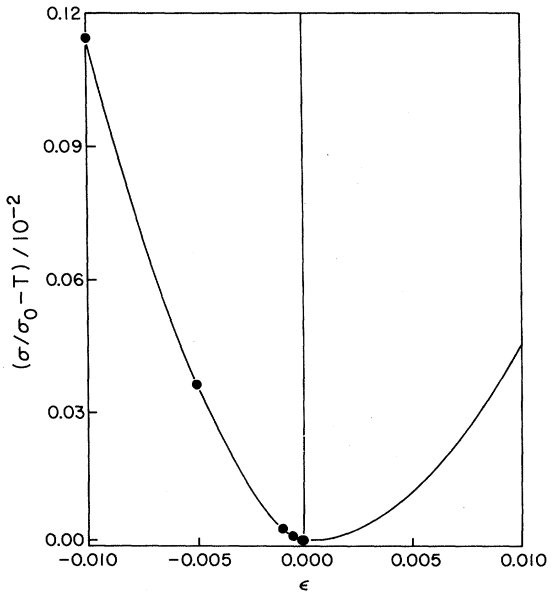

FIG. 12. Height of σ/σ_0 above the tangent line T in Fig. 11 as a function of ϵ.

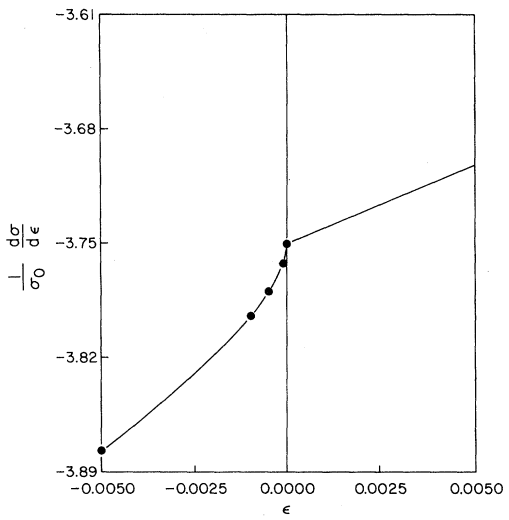

FIG. 13. $\sigma_0^{-1} d\sigma/d\epsilon$ as a function of ϵ, showing continuity of $d\sigma/d\epsilon$ at the λ point and divergence of $d^2\sigma/d\epsilon^2$ as the λ point is approached from below.

surface tension together with the numerical results from Table I. The numerical data are represented by the circles. For $\epsilon > 0$ the analytical solution is also shown. On both sides of the λ point σ/σ_0 lies above the common tangent $(1.0 - 3.75\epsilon)$, as in experiment.[2,3] To display these results with higher resolution, we show in Fig. 12 a graph of the difference between σ/σ_0 and its tangent with the ϵ scale expanded by a factor of 10 over that in Fig. 11. The curve in this plot has a horizontal tangent at the λ point, from which it deviates proportionally to $|\epsilon|^{3/2}$ or to ϵ^2 as the λ point is approached from below or from above, respectively.

The singular contribution proportional to $|\epsilon|^{3/2}$ for $T < T_\lambda$ is $|\epsilon|^\mu$, where $\mu = \frac{3}{2}$ is the mean-field-theory value of the exponent with which the tension of the interface between two phases that become identical at a critical point vanishes. When the β and γ phases are spatially separated below the critical point (as they are below an ordinary critical point in a classical fluid, although not below the λ point of helium), it is the power of $|\epsilon|$ with which $\sigma_{\beta\gamma}$ vanishes. It is related to the specific-heat and correlation-length exponents α and ν by $\mu = 2 - \nu - \alpha$ (Sec. I), or by $\mu = (d-1)\nu$ for dimensionality $d \leq 4$. The mean-field-theory value $\mu = \frac{3}{2}$ is replaced by the more accurate, nonclassical value $\mu \simeq 1.26$ at an ordinary critical point of two-phase equilibrium (in the universality class of the Ising model or of classical liquid-vapor equilibrium) or by $\mu \simeq 1.35$ at the λ point of helium and other critical points in its universality class.

It is found also in the theory of surface tension at unsymmetrical critical endpoints[8] (where the α phase is unsymmetrically related to the β and γ phases) that $|\epsilon|^\mu$ is the leading singular term. There it appears on both sides of the critical endpoint, as Hohenberg[5] supposed it would at the λ point. In the present mean-field theory we find it to occur only for $T < T_\lambda$, as Sobyanin did.[4] Whether that is a general feature of symmetrical critical endpoints (α symmetrically related to β and γ) or an artifact of the mean-field approximation, is not yet known and is an important question of principle. In any case, whether or not there is in reality a $|\epsilon|^\mu$ term at $T > T_\lambda$, we have seen that an additional $|\epsilon|^\mu$ contribution is expected below T_λ due to the vanishing, as $T \to T_\lambda$, of the superfluid order parameter $x(z)$, thus giving rise to an asymmetry in $\sigma(\epsilon)$ about $\epsilon = 0$.

To illustrate this asymmetry we show in Fig. 13 a graph of $d\sigma/d\epsilon$, the temperature derivative of the surface tension. It has a kink at the λ point. The second derivative of σ diverges as $|\epsilon|^{-1/2}$ as the λ point is approached from below but remains finite as the λ point is approached from above. The corresponding numerical data are collected in Table III. Since $d\sigma/d\epsilon$ depends on the singular contribution even more sensitively than σ does, the good agreement of the approximation $d\tilde{\sigma}/d\epsilon$ with the $d\sigma(\epsilon;n)/d\epsilon$ calculated from the numerical profiles verifies further the correctness of the expansion (7.4).

If we follow the course of the curve $d\sigma/d\epsilon$ vs ϵ in Fig. 13 upward to T_λ we see that, except for the up-

TABLE III. Temperature derivatives $d\sigma/d\epsilon$, $d\tilde{\sigma}/d\epsilon$, $d\tilde{\sigma}_x/d\epsilon$, and $d\tilde{\sigma}_y/d\epsilon$.

ϵ	$\frac{1}{\sigma_0}\frac{d\tilde{\sigma}_y}{d\epsilon}$	$\frac{1}{\sigma_0}\frac{d\tilde{\sigma}_x}{d\epsilon}$	$\frac{1}{\sigma_0}\frac{d\tilde{\sigma}}{d\epsilon}$	$\frac{1}{\sigma_0}\frac{d\sigma}{d\epsilon}$
0.0	−3.750 000	0.0	−3.750 000	−3.750 000
−0.0001	−3.750 938	−0.010 610	−3.761 548	−3.761 557
−0.0005	−3.754 688	−0.023 757	−3.778 444	−3.778 442
−0.0010	−3.759 375	−0.033 653	−3.793 028	−3.792 999
−0.0050	−3.796 875	−0.076 250	−3.873 125	−3.872 847
−0.0100	−3.843 750	−0.109 602	−3.953 352	−3.952 772
−0.0200	−3.937 500	−0.160 000	−4.097 500	−4.096 543
−0.0400	−4.125 000	−0.240 416	−4.365 416	−4.365 670
−0.0600	−4.312 500	−0.311 769	−4.624 269	−4.629 078
−0.0800	−4.500 000	−0.380 000	−4.880 000	−4.893 090
−0.1000	−4.687 500	−0.447 214	−5.134 714	−5.160 015

turn just before T_λ, it appears to be aiming toward a value less than the limiting value reached by $d\sigma/d\epsilon$ as T_λ is approached from above. It requires, as we saw, great numerical accuracy close to $\epsilon=0$ to establish the continuity of $d\sigma/d\epsilon$ there. The origin of the near discontinuity, which disappears only at the last moment as $T\to T_\lambda$, is the proximity of the exponent $\mu=\frac{3}{2}$ to unity. The nonclassical $\mu=1.35$ is enough closer to 1 for the apparent discontinuity to be even sharper when $|\epsilon|^{1.35}$ is plotted in place of $|\epsilon|^{3/2}$. This is also the origin of the discontinuity in $d\sigma/dT$ that one seems to see on viewing the Magerlein-Sanders data on an unexpanded temperature scale.

VIII. SUMMARY AND CONCLUSION

Using a two-order-parameter Landau expansion of the free-energy density in the framework of the van der Waals theory, we have calculated, both analytically and numerically, the structure of the ^{4}He liquid-vapor interface and the corresponding surface tension as a function of temperature near the λ point. We found that the thickness of the interface changes only slightly as the system passes through the λ point along the vapor pressure line, with the interfacial thickness defined as the distance over which the total density y undergoes most of its change from its bulk-liquid-phase to its bulk-gas-phase value. Accordingly, the temperature dependence of the regular part of the surface tension σ_y, which arises from the variation of the total density, is in our model analytic in ϵ and, to a good approximation, the same on both sides of the λ point. As the λ point is approached from below, the superfluid density is depleted in the interface and reaches its (diminishing) bulk-He II value only deep inside the superfluid liquid phase. The corresponding singular contribution σ_x to the surface tension vanishes proportionally to $|\epsilon|^\mu$ (where μ in this mean-field theory has the classical value $\mu=\frac{3}{2}$) as the λ point is approached from below. Such a contribution is not present above T_λ. Although it may be that a reformulated theory allowing for nonclassical values of the critical exponents would yield terms of order $|\epsilon|^\mu$ also for $\epsilon>0$, we still expect an asymmetry in the functional dependence of σ on ϵ; i.e., we expect the coefficient b in (1.2) to be in any case different on the two sides of the λ point.

It was remarked by Fisher[13] that this asymmetry could explain a puzzling detail of the data of Magerlein and Sanders.[2,3] They presented their measure-

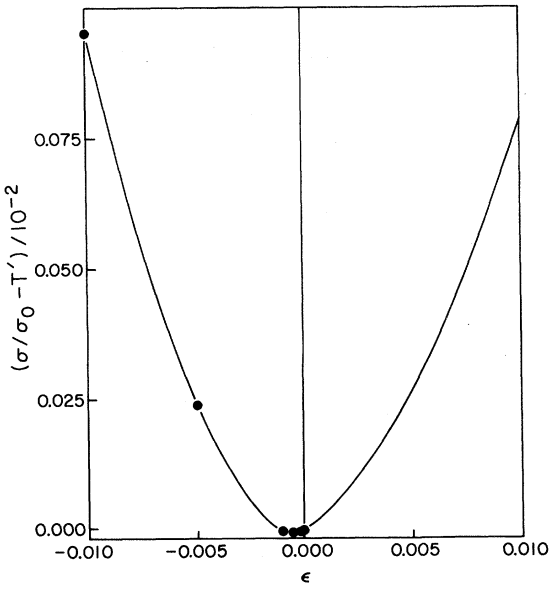

FIG. 14. Height of σ/σ_0 above the line $1.0-3.78\epsilon$ (called T') as a function of ϵ.

ments in a plot analogous to our Fig. 12, but subtracted from the surface tension a tangent that made the two branches of the resulting plot nearly symmetrical about $\epsilon=0$. In that difference plot the minimum does not occur at the λ point, as it does in our Fig. 12, but is slightly shifted towards lower temperatures. If we subtract from our σ/σ_0 data the straight line $1.0-3.78\epsilon$ instead of the tangent $1.0-3.75\epsilon$, the former being a little steeper, we obtain a difference plot, Fig. 14, that resembles the Magerlein-Sanders results much more closely than does Fig. 12; the two branches of the plot are now more nearly symmetrical, and, significantly, the minimum occurs at slightly negative ϵ.

Note added in proof. We wish to call attention to the interesting paper by V. K. Wong [J. Low Temp. Phys. 36, 629 (1979)], which treats this same problem by different methods.

ACKNOWLEDGMENTS

We are grateful to J. Kerins and M. Robert for illuminating and helpful discussions, and to the Max-Planck-Gesellschaft zur Förderung der Wissenschaften for the award of an Otto-Hahn fellowship. This work was supported by the National Science Foundation and the Cornell University Materials Science Center.

---

*Present address: Physik-Department der Technischen Universität München, James-Franck-Strasse, 8046 Garching, West Germany.

[1]R. B. Griffiths, Phys. Rev. Lett. 24, 715 (1970); E. G. D. Cohen, in *Fundamental Problems in Statistical Mechanics III*, edited by E. G. D. Cohen (North-Holland, Amsterdam, 1975), pp. 47–79.

[2]J. H. Magerlein and T. M. Sanders, Jr., Phys. Rev. Lett. 36, 258 (1976).

[3]J. H. Magerlein, Ph.D. thesis, University of Michigan, 1975 (unpublished).

[4]A. A. Sobyanin, Zh. Eksp. Teor. Fiz. 61, 433 (1971) [Sov. Phys.—JETP 34, 229 (1972)].

[5]P. C. Hohenberg, J. Low Temp. Phys. 13, 433 (1973).

[6]J. D. van der Waals, Z. Phys. Chem. (Leipzig) 13, 657 (1894); J. S. Rowlinson, J. Stat. Phys. 20, 197 (1979).

[7]J. W. Cahn and J. E. Hilliard, J. Chem. Phys. 28, 258 (1958).

[8]F. Ramos Gómez and B. Widom, Physica (Utrecht) 104A, 595 (1980).

[9]B. Widom, Physica (Utrecht) 95A, 1 (1979).

[10]The numerical method was originally developed by J. Kerins [Ph.D. thesis, Cornell University, 1982 (unpublished)] for the calculation of surface and line tensions of noncritical fluid phases. We have generalized this method to include two disparate length scales, one of them diverging, and we have improved the method's accuracy so that it can treat subtle effects near the critical endpoint.

[11]The inequality $\sigma_f<\sigma_k$ may be reversed by a choice $\tau\gtrsim 0.75$, as may be understood qualitatively from (6.7)–(6.11).

[12]F. Ramos Gómez, Sc. D. thesis, Universidad Nacional Autónoma de México, 1980 (unpublished); M. Robert and P. Tavan, J. Chem. Phys. (in press).

[13]M. E. Fisher (private communication).